  Bull. Chem. Soc. Jpn., 57, 1116—1122 (1984) [Vol. 57, No. 4

# Copper(II)-Catalyzed Transamination of Hydrophobic Pyridoxamine with Pyruvic Acid in Functionalized Bilayer Vesicles†

Yukito MURAKAMI,* Jun-ichi KIKUCHI, Akio NAKANO,†† Kazunari AKIYOSHI, and Toru IMORI
*Department of Organic Synthesis, Faculty of Engineering, Kyushu University, Hakozaki, Higashi-ku, Fukuoka 812*
(Received October 26, 1983)

The copper(II)-catalyzed transamination of 2-methyl-3-hydroxy-4-aminomethyl-5-(dodecylthiomethyl)pyridine ($C_{12}$SPM) with sodium pyruvate was investigated in an aqueous medium at pH 6.8, $\mu$ 0.10 (KCl), and 30.0 ±0.1 °C in the presence of molecular aggregates of *N,N*-ditetradecyl-$N^{\alpha}$-[6-(trimethylammonio)hexanoyl]-L-alaninamide bromide ($N^+C_5$Ala2$C_{14}$), *N,N*-ditetradecyl-$N^{\alpha}$-[6-(trimethylammonio)hexanoyl]-L-histidinamide bromide ($N^+C_5$His2$C_{14}$), or hexadecyltrimethylammonium bromide (CTAB). The reaction afforded the corresponding pyridoxal analogue ($C_{12}$SPL) and alanine as the final products upon addition of edta which liberates the copper(II) ion from the coordination sites of the aldimine Schiff-base. The coordination interaction between the copper(II) ion and $C_{12}$SPM, which takes place prior to the transamination, was clarified by electronic spectroscopy. The reactivity of the 2:1 (ketimine:$Cu^{II}$) complex was found to be much larger than that of the 1:1 complex in the molecular assemblies of $N^+C_5$Ala2$C_{14}$ and CTAB, and the formation of the former species was more pronounced in the $N^+C_5$Ala2$C_{14}$ vesicle. The bilayer vesicle formed with $N^+C_5$His2$C_{14}$ allowed the formation of the 1:1 complex in preference to that of the 2:1 complex, and the coordination-free imidazolyl group of the amphiphile effectively catalyzed the isomerization as a general base.

Pyridoxal-5′-phosphate (PLP) is known to catalyze various transformation reactions of amino acids such as transamination, elimination, racemization, and decarboxylation as the coenzyme in biological systems.[1] Although most of the PLP-dependent enzymatic reactions can be simulated by nonenzymatic systems,[2] such nonenzymatic reactions are much less efficient than the corresponding enzymatic ones with respect to reactivity, substrate specificity, and reaction selectivity. In order to improve the catalytic efficiency of model systems for the PLP-dependent enzymes, micellar surfactants,[3] synthetic polymers,[4] and macrocyclic compounds[5] have been utilized in recent years to simulate the functions of apoenzymes. We have reported previously that a bilayer membrane composed of a synthetic peptide lipid can provide a reaction field favorable for the transamination of PLP with a hydrophobic amino acid.[6]

In the present work, we prepared hydrophobic vitamin $B_6$ analogues, $C_{12}$SPM and $C_{12}$SPL, and investigated the reaction of $C_{12}$SPM with pyruvate in single-walled vesicles of $N^+C_5$Ala2$C_{14}$ and $N^+C_5$His2$C_{14}$ as effected by the copper(II) ion. The kinetic behavior of the transamination reaction was analyzed in the light of metal-coordination modes observed for $C_{12}$SPM and its ketimine Schiff-base with the copper(II) ion. The kinetic effect of single-walled vesicles formed with $N^+C_5$His2$C_{14}$ on the transamination is to be discussed in view of the base catalysis of the histidyl residue.

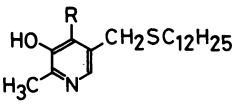

$C_{12}$SPM (R = $CH_2NH_2$)
$C_{12}$SPL (R = CHO)

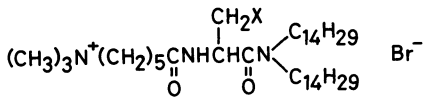

$N^+C_5$Ala2$C_{14}$ (X = H)
$N^+C_5$His2$C_{14}$ (X =  )

## Experimental

Spectroscopic data were taken on a Union Giken SM-401 UV-visible spectrophotometer and a Hitachi R-24B NMR spectrometer. pH-Measurements were carried out with a Beckman expandomatic SS-2 pH meter equipped with a Metrohm EA-125 combined electrode after calibration with a combination of appropriate standard aqueous buffers. Melting points were measured with a Yanaco MP-S1 apparatus (hot-plate type). Elemental analyses were performed at the Microanalysis Center of Kyushu University.

Hexadecyltrimethylammonium bromide (CTAB) of Nakarai Chemicals was recrystallized from ethanol, mp 237—239 °C (decomp). *N,N*-Ditetradecyl-$N^{\alpha}$-[6-(trimethylammonio)hexanoyl]-L-alaninamide bromide ($N^+C_5$Ala2$C_{14}$) and *N,N*-ditetradecyl-$N^{\alpha}$-[6-(trimethylammonio)hexanoyl]-L-histidinamide bromide ($N^+C_5$His2$C_{14}$) were prepared as described elsewhere.[6,7] 2-Methyl-3-hydroxy-4-aminomethyl-5-(dodecylthiomethyl)pyridine dihydrobromide ($C_{12}$SPM·2HBr) and 2-methyl-3-hydroxy-4-formyl-5-(dodecylthiomethyl)pyridine ($C_{12}$SPL) were prepared as described below.

*2-Methyl-3-hydroxy-4-aminomethyl-5-(bromomethyl)pyridine Dihydrobromide (PMBr).* Pyridoxamine dihydrochloride (1.0 g, 4.2 mmol) dissolved in 48% aqueous hydrobromic acid (25 ml) was refluxed for 2 h. After the mixture was evaporated to dryness *in vacuo*, the crude product was dissolved in methanol and purified by reprecipitation with ether; yield 1.3 g (81%), mp 265—270 °C (decomp).

*2-Methyl-3-hydroxy-4-aminomethyl-5-(dodecylthiomethyl)pyridine Dihydrobromide ($C_{12}$SPM·2HBr).* A solution of 1-dodecanethiol (530 mg, 2.6 mmol) in dry ethanol (5 ml) was added dropwise to 50 mg of sodium metal dissolved in dry ethanol (5 ml) with stirring under nitrogen atmosphere. PMBr (400 mg, 1.0 mmol) dissolved in dry ethanol (50 ml) was added dropwise to the resulting mixture with stirring under nitrogen at 0 °C. The mixture was evaporated to dryness *in*

† Contribution No. 716 from this Department.
†† Present address: Department of Food Science, Toa University, Shimonoseki, Yamaguchi 751.

*vacuo*, and the residue was recrystallized from methanol. The crude product dissolved in methanol was treated with 48% aqueous hydrobromic acid, evaporated to dryness, and purified by gel-filtration chromatography on columns of Toyopearl HW-40 fine and Sephadex LH-20 in this sequence with methanol as an eluant to afford a white solid: yield 0.17 g (33%), mp 193— 194 °C (decomp); $^1$H-NMR ($CD_3OD$, TMS) $\delta$=0.88 [3H, t, $S(CH_2)_{11}\underline{CH_3}$], 1.27 [20H, m, $SCH_2(\underline{CH_2})_{10}CH_3$], 2.50 [2H, t, $S\underline{CH_2}(CH_2)_{10}CH_3$], 2.67 [3H, s, 2-$\underline{CH_3}$ on pyridine ring], 3.96 [2H, s, $\underline{CH_2}S(CH_2)_{11}CH_3$], 4.39 [2H, s, $\underline{CH_2}NH_3^+$], and 8.16 [1H, s, 6-$\underline{H}$ on pyridine ring].

Found: C, 47.15; H, 7.72; N, 5.66%. Calcd for $C_{20}H_{36}N_2OS \cdot 2HBr$: C, 46.70; H, 7.45; N, 5.45%.

*2-Methyl-3-hydroxy-4-formyl-5-(dodecylthiomethyl)pyridine ($C_{12}$SPL).* A mixture of potassium hydroxide (1.37 g, 9.8 mmol), $C_{12}$SPM·2HBr (0.10 g, 0.19 mmol), $\alpha$-oxoglutaric acid (1.46 g, 10 mmol), and zinc nitrate (0.116 g, 0.39 mmol) in methanol (200 ml) was stirred for 24 h at room temperature, and evaporated to dryness *in vacuo*. The residue was suspended in 2 mol dm$^{-3}$ aqueous hydrochloric acid (100 ml), and extracted with chloroform (3 × 50 ml). The chloroform extract was washed with water, dried over anhydrous sodium sulfate, and evaporated to dryness *in vacuo*. The crude product was purified by gel-filtration chromatography on a column of Sephadex LH-20 with methanol as an eluant to afford a pale yellow oil: yield 29 mg (39%); $^1$H-NMR ($CDCl_3$, TMS) $\delta$=0.89 [3H, t, $S(CH_2)_{11}\underline{CH_3}$], 1.29 [20H, m, $SCH_2(\underline{CH_2})_{10}CH_3$], 2.35 [2H, br s, $S\underline{CH_2}(CH_2)_{10}CH_3$], 2.51 [3H, s, 2-$\underline{CH_3}$ on pyridine ring], 3.90 [2H, s, $\underline{CH_2}S(CH_2)_{11}CH_3$], 7.87 [1H, s, 6-H on pyridine ring], and 10.45 [1H, s, CHO].

Found: C, 68.06; H, 9.46; N, 4.01%. Calcd for $C_{20}H_{33}NO_2S$: C, 68.34; H, 9.46; N, 3.98%.

*Kinetic Measurements.* The reaction medium was prepared as follows. (i) An appropriate amount of the stock solution of one of the amphiphiles ($N^+C_5Ala2C_{14}$, $N^+C_5His2C_{14}$, and CTAB) in ethanol was placed in a glass vessel, and evaporated *in vacuo* to remove the solvent completely. An aqueous HEPES (2-[4-(2-hydroxyethyl)-1-piperazinyl]ethanesulfonic acid) buffer (2.5 mmol dm$^{-3}$, pH 6.8) containing 0.1 mol dm$^{-3}$ potassium chloride was added to the residue. (ii) An aqueous dispersion of the amphiphile thus prepared was sonicated for 2 min with a probe-type sonicator at 30-W power (W-220F, Heat Systems-Ultrasonics). The resulting vesicle solution was sufficiently clear and gave good kinetic reproducibility. Each run was initiated by adding 20 µl of an aqueous solution of $C_{12}$SPM ($5.0 \times 10^{-3}$ mol dm$^{-3}$), an appropriate quantity of an aqueous solution of $Cu(ClO_4)_2$ which was standardized by conventional chelatometric titration ($1.0 \times 10^{-2}$ mol dm$^{-3}$), and 100 µl of a freshly prepared aqueous solution of sodium pyruvate (0.1 mol dm$^{-3}$) to 2.0 ml of the reaction medium which was pre-equilibrated at 30.0 ± 0.1 °C in a thermostated cell set in the spectrophotometer.

## Results and Discussion

*Spectral Change in the Course of Transamination.* The transamination reaction of $C_{12}$SPM with sodium pyruvate, as effected by the presence of single-walled vesicles of $N^+C_5Ala2C_{14}$ and $N^+C_5His2C_{14}$ as well as by CTAB micelles, was followed spectrophotometrically in the aqueous HEPES buffer at pH 6.8, $\mu$ 0.10 (KCl), and 30.0 ± 0.1 °C. Figure 1 shows the spectral change observed along the progress of transamination in the presence of the $N^+C_5Ala2C_{14}$ vesicle. The absorption spectrum of $C_{12}$SPM in the single-walled vesicle shows a maximum at 293 nm and a shoulder at 315 nm. This indicates the presence of two species which are different in protonation site from each other (Scheme 1).[8,9] The charged form ($PM_1$) was primarily observed in dioxane–water (1:9 v/v), and the fraction of the neutral

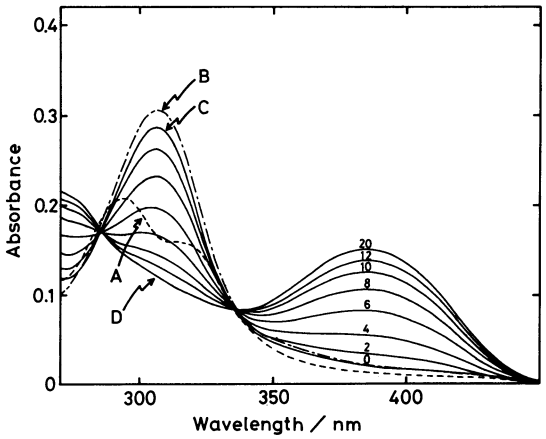


Fig. 1. Spectral change along the progress of transamination of $C_{12}$SPM ($5.0 \times 10^{-5}$ mol dm$^{-3}$) with sodium pyruvate ($5.0 \times 10^{-3}$ mol dm$^{-3}$) in the presence of $Cu(ClO_4)_2$ ($5.0 \times 10^{-5}$ mol dm$^{-3}$) and $N^+C_5Ala2C_{14}$ vesicle ($1.0 \times 10^{-3}$ mol dm$^{-3}$) in an aqueous HEPES buffer ($2.5 \times 10^{-3}$ mol dm$^{-3}$) at pH 6.8, $\mu$ 0.10 (KCl), and 30.0 ± 0.1 °C: A, $C_{12}$SPM alone; B, $Cu^{II}$–$C_{12}$SPM species; C, $Cu^{II}$– ketimine species; D, $Cu^{II}$–aldimine species. Nunerals refer to reaction periods (in min) for the ketimine–aldimine isomerization.

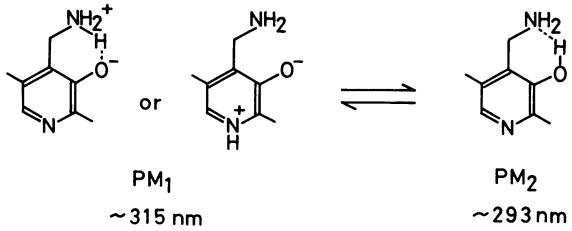


Scheme 1.

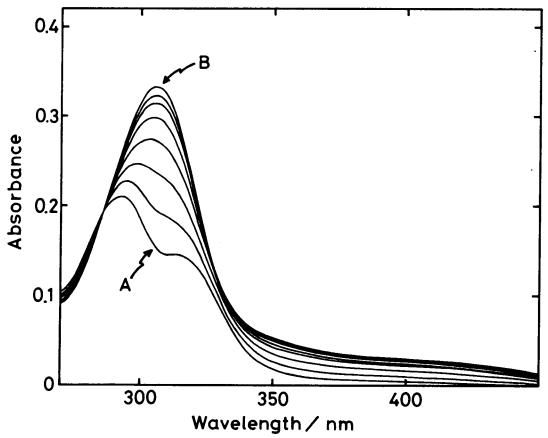


Fig. 2. Electronic absorption spectra of $C_{12}$SPM ($5.0 \times 10^{-5}$ mol dm$^{-3}$) in an aqueous HEPES buffer ($2.5 \times 10^{-3}$ mol dm$^{-3}$) at pH 6.8, $\mu$ 0.10 (KCl), and 30.0 ± 0.1 °C in the presence of $N^+C_5Ala2C_{14}$ vesicle ($1.0 \times 10^{-3}$ mol dm$^{-3}$) and varying amounts of $Cu(ClO_4)_2$: 0, $5.1 \times 10^{-6}$, $1.0 \times 10^{-5}$, $1.5 \times 10^{-5}$, $2.0 \times 10^{-5}$, $2.5 \times 10^{-5}$, $3.0 \times 10^{-5}$, and $5.0 \times 10^{-5}$ mol dm$^{-3}$ (read from A to B).

form ($PM_2$) increased with an increase in dioxane content. The microenvironmental polarity for the pyridoxamine moiety of $C_{12}$SPM in the aggregates was evaluated from the relative intensities of the absorption maxima for these species. As a result, both vesicular and micellar systems provide a microenvironment equivalent to that provided by dioxane–water (1:1 v/v) (Kosower's Z-value, 87).[10] Addition of $Cu(ClO_4)_2$ resulted in an immediate shift of the absorption maximum to 306 nm along with an increase in intensity as shown in Fig. 2. This spectral change is analogous to that observed for the formation of the $Cu^{II}$–pyridoxamine complex in methanol[9] and attributed to the formation of the $Cu^{II}$–$C_{12}$SPM complex (**1** in Scheme 2). Subsequently, the ketimine Schiff-base complex (**2** in Scheme 2), having an absorption maximum at 305 nm, was formed instantaneously upon addition of sodium pyruvate to the solution. The intensity of this peak decreased with time, isosbestic points being observed at 286 and 335 nm. A new absorption band appeared at 385 nm and increased in intensity as the reaction proceeded. The absorption spectrum observed at the final stage of reaction was identical with that of the copper complex of the aldimine Schiff-base of $C_{12}$SPL formed with alanine (**3** in Scheme 2). When an aqueous solution of tetrasodium ethylenediaminetetraacetate (edta; 10-fold molar excess over $Cu^{II}$ ion) was added to the final solution, the spectrum changed immediately indicating the formation of the metal-free aldimine Schiff-base of $C_{12}$SPL formed with alanine. This Schiff-base was hydrolyzed to $C_{12}$SPL and alanine completely within 1 h. The isomerization of the ketimine Schiff-base to the corresponding aldimine was not observed in the absence of $Cu(ClO_4)_2$. Similar reaction behavior was found in other amphiphile systems of the present study. Table 1 summarizes the spectral parameters for various species formed in the present amphiphile systems.

In the light of these observations, the overall reaction pathway is explicitly given in Scheme 2. Matsumoto *et al.* reported that the reaction of pyridoxamine with

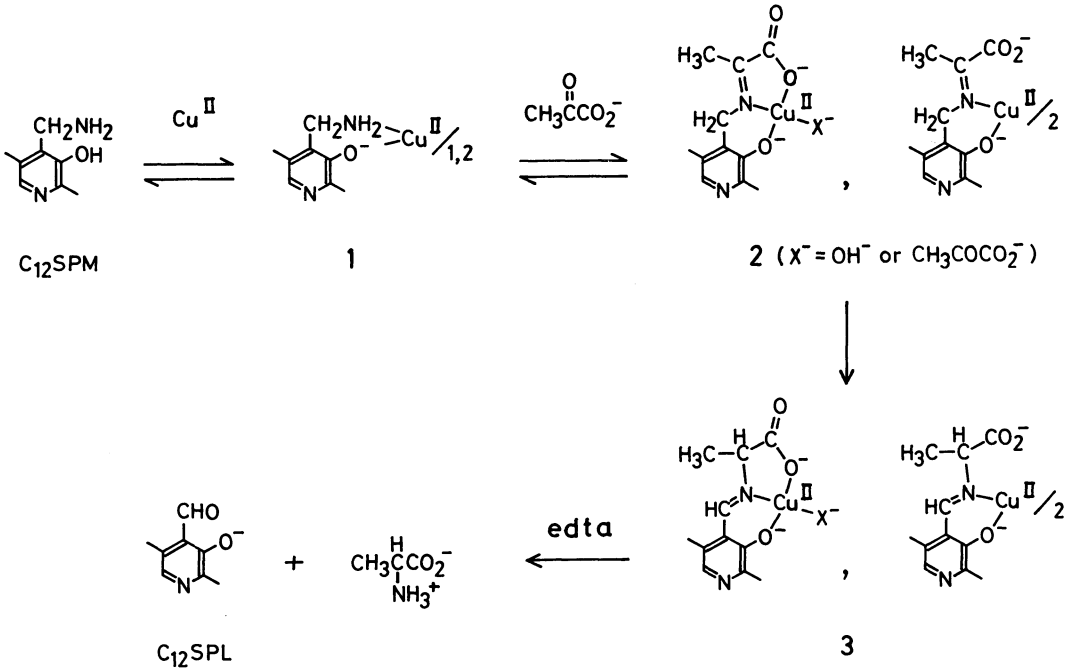


Scheme 2.

Table 1. Spectral parameters[a] for chemical species involved in the $Cu^{II}$-catalyzed transamination of $C_{12}$SPM with sodium pyruvate in various amphiphile systems at 30.0±0.1 °C[b]

| Species[c] | Amphiphile | | |
|---|---|---|---|
| | $N^+C_5Ala2C_{14}$ | $N^+C_5His2C_{14}$ | CTAB |
| $C_{12}$SPM | 293 ($4.2\times10^3$)<br>315sh ($3.1\times10^3$) | 294 ($4.2\times10^3$)<br>315sh ($3.1\times10^3$) | 295 ($3.9\times10^3$)<br>314sh ($3.7\times10^3$) |
| $Cu^{II}$-$C_{12}$SPM (**1**) | 306 | 309 | 305 |
| $Cu^{II}$-KSB (**2**) | 305 | 307 | 304 |
| $Cu^{II}$-ASB (**3**) | 385 | 392 | 388 |

a) Wavelengths (nm) at absorption maxima. Molar absorption coefficients are given in parentheses. b) Cationic amphiphile systems in an aqueous HEPES buffer ($2.5\times10^{-3}$ mol dm$^{-3}$) at pH 6.8 and $\mu$ 0.10 (KCl): $N^+C_5Ala2C_{14}$, $1.0\times10^{-3}$ mol dm$^{-3}$; $N^+C_5His2C_{14}$, $1.0\times10^{-3}$ mol dm$^{-3}$; CTAB, $3.0\times10^{-3}$ mol dm$^{-3}$. Initial concentrations of reactants: $C_{12}$SPM, $5.0\times10^{-5}$ mol dm$^{-3}$; $Cu(ClO_4)_2$, $5.0\times10^{-5}$ mol dm$^{-3}$; sodium pyruvate, $5.0\times10^{-3}$ mol dm$^{-3}$. c) For structures of metal complexes, see Scheme 2; KSB, ketimine Schiff-base; ASB, aldimine Schiff-base.

α-keto acids and copper(II) ion yielded the $Cu^{II}$–aldimine chelates in methanol, but the rate-determining step was not unambiguously defined.[11] In the present transamination reaction, however, the isomerization of the $Cu^{II}$–ketimine chelate to the $Cu^{II}$–aldimine chelate is exclusively the rate-determining step without any ambiguity, since the reaction time course was not influenced by the mixing mode of the reactants, simultaneous or sequential, and showed a monophasic kinetic feature. The absorption bands characteristic of the $Cu^{II}$–ketimine and –aldimine chelates were used to determine the rates of isomerization reaction.

*Metal-coordination Behavior of $C_{12}$SPM.* Prior to the transamination reaction, the copper(II) ion undergoes coordination with $C_{12}$SPM as shown in Scheme 2. The $\pi$–$\pi^*$ transition bands appearing in the 300-nm range are due to the pyridoxamine chromophore of $C_{12}$SPM in the $N^+C_5$Ala2$C_{14}$ vesicle, and their intensities increased upon addition of $Cu(ClO_4)_2$ (Fig. 2). The simplest coordination equilibrium would involve the formation of the 1:1 ($C_{12}$SPM:$Cu^{II}$) complex (Eq. 1).

$$C_{12}SPM + Cu^{II} \rightleftharpoons Cu^{II}(C_{12}SPM) \quad (1)$$

This is not the case, however, since the value of $[Cu^{II}(C_{12}SPM]/[C_{12}SPM][Cu^{II}]$ varied as the concentration of $Cu(ClO_4)_2$ was changed. Alternatively, the copper-coordination scheme, which involves the formation of both 2:1 and 1:1 ($C_{12}$SPM:$Cu^{II}$) complexes (Eq. 2), was utilized to analyze the equilibrium data.

$$2(C_{12}SPM) \underset{K_1}{\overset{Cu^{II}}{\rightleftharpoons}} Cu^{II}(C_{12}SPM)_2 \underset{K_2}{\overset{Cu^{II}}{\rightleftharpoons}} 2\,Cu^{II}(C_{12}SPM) \quad (2)$$

The formation of such 2:1 and 1:1 chelate species has been also reported for the coordination of $Cu^{II}$ ion with pyridoxamine in aqueous media.[12] The observation of an isosbestic point at 286 nm (Fig. 2) assures that the present 2:1 and 1:1 chelates have an identical molar absorption coefficient as given in terms of the $C_{12}$SPM unit. Now, the respective stability constants ($K_1$ and $K_2$), defined by Eqs. 3 and 4, were evaluated by the least-squares analysis in a manner similar to that applied to the zinc(II)–paracyclophane system.[13]

$$K_1 = \frac{[Cu^{II}(C_{12}SPM)_2]}{[C_{12}SPM]^2[Cu^{II}]} \quad (3)$$

$$K_2 = \frac{[Cu^{II}(C_{12}SPM)]^2}{[Cu^{II}(C_{12}SPM)_2][Cu^{II}]} \quad (4)$$

The total concentration of $C_{12}$SPM bound to $Cu^{II}$ at a given concentration of $Cu(ClO_4)_2$ ($c$=$[Cu^{II}(C_{12}SPM)]$+ $2[Cu^{II}(C_{12}SPM)_2]$) is calculated by Eq. 5.

$$c = \frac{\Delta A}{A_c - A_f}[C_{12}SPM]_0 \quad (5)$$

Here, $A_c$ and $A_f$ denote the absorbance in the presence of sufficiently excess $Cu(ClO_4)_2$ and that in its absence, respectively, at a selected wavelength close to the absorption maxima of the $Cu^{II}$–$C_{12}$SPM complexes; $\Delta A$ is the absorbance change with respect to $A_f$ at the intermediate concentration range of $Cu(ClO_4)_2$; and $[C_{12}SPM]_0$ denotes the total concentration of $C_{12}$SPM. Combining Eqs. 3, 4, and 5, we obtain Eq. 6.

$$(K_1K_2)^{1/2}[C_{12}SPM]([Cu^{II}]_0 - c) + K_1[C_{12}SPM]^2(2[Cu^{II}]_0 - c) = c \quad (6)$$

Here, $[Cu^{II}]_0$ is the initial concentration of $Cu(ClO_4)_2$. This equation is in the form, $aX + bY = Z$, where $a$ and $b$ are $(K_1K_2)^{1/2}$ and $K_1$, respectively, and $X$, $Y$, and $Z$ are experimentally observable. $K_1$ and $K_2$ were determined by the least-squares analysis using all the experimental sets of ($X$, $Y$, $Z$) at various concentrations of $Cu(ClO_4)_2$. The results are summarized in Table 2. The observed total concentration of $C_{12}$SPM bound to $Cu^{II}$ was computationally reproduced quite satisfactorily by the aid of the $K_1$ and $K_2$ values determined as above for the whole concentration range of $Cu(ClO_4)_2$ employed in the present study (Fig. 3).

Figure 4 shows the calculated molar distributions of the 2:1 and 1:1 chelate species of $C_{12}$SPM in the three different molecular assemblies as a function of the $Cu^{II}$ concentration. In both $N^+C_5$Ala2$C_{14}$ vesicle and CTAB micelle, the fraction of the 2:1 complex is greater than that of the 1:1 complex in a low concentration range of $Cu^{II}$, while the fraction of the latter exceeds that of the former at higher $Cu^{II}$ concentrations. Meanwhile, the

Table 2. Stability constants for copper(II) complexes of $C_{12}$SPM in various amphiphile systems at 30.0±0.1 °C[a]

| | $N^+C_5$Ala2$C_{14}$ | $N^+C_5$His2$C_{14}$ | CTAB |
|---|---|---|---|
| $K_1$/mol$^{-2}$ dm$^6$ | $3.0\times10^{10}$ | $1.8\times10^{10}$ | $1.1\times10^{11}$ |
| $K_2$ | 0.26 | 320 | 42 |

a) Cationic amphiphile systems in an aqueous HEPES buffer ($2.5\times10^{-3}$ mol dm$^{-3}$) at pH 6.8 and $\mu$ 0.10 (KCl): $N^+C_5$Ala2$C_{14}$, $1.0\times10^{-3}$ mol dm$^{-3}$; $N^+C_5$His2$C_{14}$, $1.0\times10^{-3}$ mol dm$^{-3}$; CTAB, $3.0\times10^{-3}$ mol dm$^{-3}$.

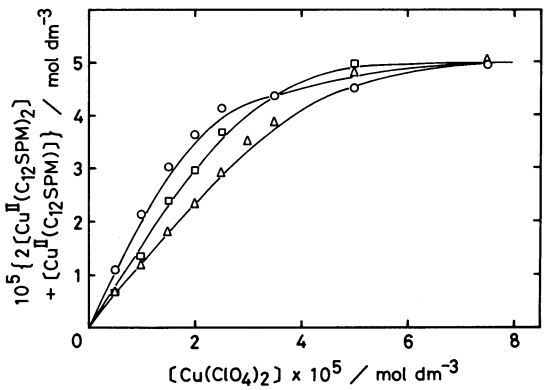


Fig. 3. Correlations between total concentrations of $Cu(ClO_4)_2$ and $Cu^{II}$-$C_{12}$SPM complexes in an aqueous HEPES buffer ($2.5\times10^{-3}$ mol dm$^{-3}$) at pH 6.8, $\mu$ 0.10 (KCl), and 30.0±0.1 °C in the presence of $N^+C_5$Ala2$C_{14}$ (○, $1.0\times10^{-3}$ mol dm$^{-3}$), $N^+C_5$His2$C_{14}$ (△, $1.0\times10^{-3}$ mol dm$^{-3}$), and CTAB (□, $3.0\times10^{-3}$ mol dm$^{-3}$). Solid lines refer to the calculated data by the aid of evaluated stability constants ($K_1$ and $K_2$, Table 2); total concentration of $C_{12}$SPM, $5.0\times10^{-5}$ mol dm$^{-3}$.

1:1 complex is formed predominantly over the whole concentration range of $Cu(ClO_4)_2$ in the $N^+C_5His2C_{14}$ vesicle. This result strongly indicates that the imidazolyl group of $N^+C_5His2C_{14}$ undergoes coordination with the copper(II) ion which leads to the formation of the 1:1 complex in preference to that of the 2:1 complex.[14]

*Kinetic Behavior of Isomerization Reaction.* The isomerization of the $Cu^{II}$-ketimine Schiff-base to the corresponding $Cu^{II}$-aldimine chelate was followed by means of electronic absorption spectroscopy at $30.0 \pm 0.1$ °C in the presence of cationic amphiphiles.

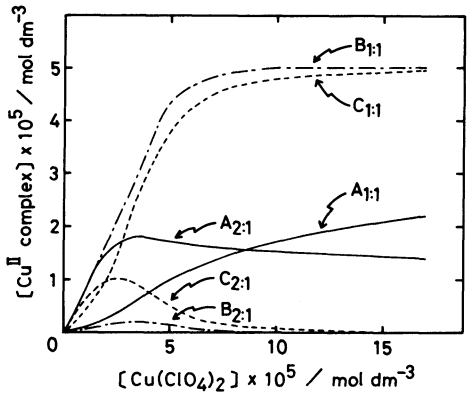


Fig. 4. Distributions of $Cu^{II}$-$C_{12}SPM$ complexes in an aqueous HEPES buffer ($2.5\times10^{-3}$ mol dm$^{-3}$) at pH 6.8, $\mu$ 0.10 (KCl), and $30.0\pm0.1$ °C in the presence of $N^+C_5Ala2C_{14}$ (A, $1.0\times10^{-3}$ mol dm$^{-3}$), $N^+C_5His2C_{14}$ (B, $1.0\times10^{-3}$ mol dm$^{-3}$), and CTAB (C, $3.0\times10^{-3}$ mol dm$^{-3}$). Subscripts 1:1 and 2:1 denote the 1:1 and 2:1 ($C_{12}SPM$:$Cu^{II}$) complexes, respectively; total concentration of $C_{12}SPM$, $5.0\times10^{-5}$ mol dm$^{-3}$.

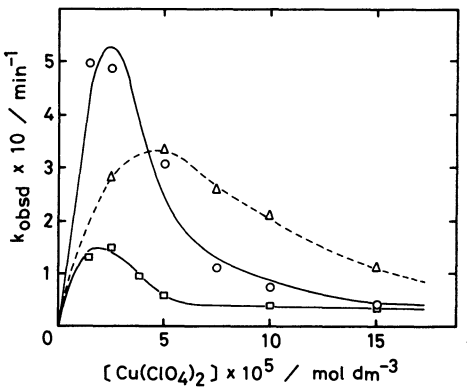


Fig. 5. Correlations between total concentration of $Cu(ClO_4)_2$ and first-order rate constant for the isomerization of $Cu^{II}$-ketimine to $Cu^{II}$-aldimine in an aqueous HEPES buffer ($2.5\times10^{-3}$ mol dm$^{-3}$) at pH 6.8, $\mu$ 0.10(KCl), and $30.0\pm0.1$ °C in the presence of $N^+C_5Ala2C_{14}$ (○, $1.0\times10^{-3}$ mol dm$^{-3}$), $N^+C_5His2C_{14}$ (△, $1.0\times10^{-3}$ mol dm$^{-3}$), and CTAB (□ $3.0\times10^{-3}$ mol dm$^{-3}$) with initial concentrations: $C_{12}SPM$, $5.0\times10^{-5}$ mol dm$^{-3}$; sodium pyruvate, $5.0\times10^{-3}$ mol dm$^{-3}$. Solid lines refer to the calculated data on the basis of Eq. 7 and evaluated kinetic parameters (Table 3).

The absorbance increase due to the formation of the $Cu^{II}$-aldimine chelate was monitored at 385 nm to determine the reaction rate. The observed rate constant, $k_{obsd}$, was plotted against the total concentration of $Cu(ClO_4)_2$ as shown in Fig. 5.

In both $N^+C_5Ala2C_{14}$ vesicle and CTAB micelle, the rate constant reaches a maximum and then falls down sharply as the $Cu^{II}$ concentration increases. This overall feature is completely reproducible in several sets of kinetic runs. In the light of the coordination behavior of $C_{12}SPM$ with the copper(II) ion, it can be considered that the copper-binding scheme for the formation of $Cu^{II}$-ketimine Schiff-base complexes involves both 2:1 and 1:1 (ketimine:$Cu^{II}$) chelate species as shown in Scheme 2. The observed correlations given in Fig. 5 can be reproduced by summing up the reaction rates of both 1:1 and 2:1 complexes; the former and latter complexes are designated as $Cu^{II}(KSB)$ and $Cu^{II}(KSB)_2$ with specific rate constants, $k_1$ and $k_2$ (per ketimine Schiff-base), respectively. The specific rate constant for the metal-free ketimine Schiff-base is neglected under the present conditions. The kinetic expression, on the basis of Scheme 3, is given by Eq. 7, where $[Cu^{II}\text{-KSB}]_T$ is the total concentration of the $Cu^{II}$-ketimine chelates as given in terms of the ketimine Schiff-base unit.

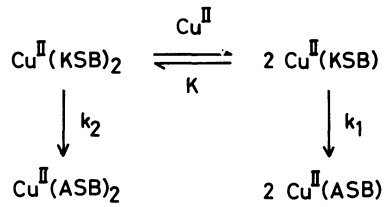


KSB : ketimine Schiff-base
ASB : aldimine Schiff-base

Scheme 3.

$$k_{obsd}[Cu^{II}\text{-KSB}]_T = k_1[Cu^{II}(KSB)] + 2k_2[Cu^{II}(KSB)_2] \quad (7)$$

The concentrations of $Cu^{II}(KSB)$ and $Cu^{II}(KSB)_2$ are interrelated by the stability constant ($K$) defined by Eq. 8.

$$K = \frac{[Cu^{II}(KSB)]^2}{[Cu^{II}(KSB)_2][Cu^{II}]} \quad (8)$$

The determination of $K$ values was not made by the spectral method which was applied to the $Cu^{II}$-$C_{12}SPM$ system, because the coordination behavior given by Eq. 8 is accompanied with the isomerization reaction. Accordingly, the values of $k_1$, $k_2$, and $K$ were obtained by the regression analysis which minimizes the sum of the squares of errors ($U$) applied to all the experimental data (Eq. 9).

$$U = \sum \{k_{obsd}[Cu^{II}\text{-KSB}]_T - k_1[Cu^{II}(KSB)] - 2k_2[Cu^{II}(KSB)_2]\}^2 \quad (9)$$

The value of $[Cu^{II}\text{-KSB}]_T$ was evaluated from the final concentration of the $Cu^{II}$-aldimine Schiff-base

Table 3. Specific rate constants for isomerization reaction of $Cu^{II}$-ketimine to $Cu^{II}$-aldimine and stability constants for $Cu^{II}$-ketimine chelates in amphiphile systems at 30.0±0.1 °C[a)]

| Parameter | Amphiphile | |
|---|---|---|
| | $N^+C_5Ala2C_{14}$ | CTAB |
| $k_1/min^{-1}$ | 0.041 | 0.036 |
| $k_2/min^{-1}$ | 0.70 | 0.17 |
| $K$ | 20 | 130 |

a) Cationic amphiphile systems in an aqueous buffer ($2.5\times10^{-3}$ mol $dm^{-3}$) at pH 6.8 and $\mu$ 0.10 (KCl); $N^+C_5Ala2C_{14}$, $1.0\times10^{-3}$ mol $dm^{-3}$; CTAB, $3.0\times10^{-3}$ mol $dm^{-3}$.

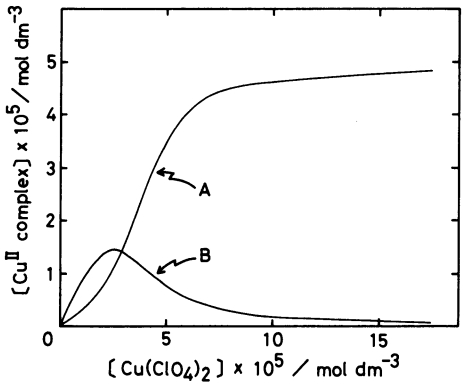


Fig. 6. Distributions of $Cu^{II}$-ketimine chelates in an aqueous HEPES buffer ($2.5\times10^{-3}$ mol $dm^{-3}$) at pH 6.8, $\mu$ 0.10 (KCl), and 30.0±0.1 °C in the presence of $N^+C_5Ala2C_{14}$ vesicle ($1.0\times10^{-3}$ mol $dm^{-3}$): A, 1:1 (ketimine:$Cu^{II}$) chelate; B, 2:1 chelate. Initial concentrations: $C_{12}SPM$, $5.0\times10^{-5}$ mol $dm^{-3}$; sodium pyruvate, $5.0\times10^{-3}$ mol $dm^{-3}$.

produced by the isomerization reaction,[15)] since the $Cu^{II}$-ketimine chelate was quantitatively converted into the corresponding $Cu^{II}$-aldimine chelate.

The kinetic parameters thus obtained for the isomerization carried out in the aggregates of $N^+C_5Ala2C_{14}$ and CTAB are listed in Table 3, and the calculated molar distributions of individual chelate species in the $N^+C_5Ala2C_{14}$ vesicle are shown in Fig. 6 as a function of the $Cu^{II}$ concentration. In a manner as observed for the $Cu^{II}$-$C_{12}SPM$ system, the fraction of the 2:1 complex is greater than that of the 1:1 complex in a low $Cu^{II}$ concentration range. However, the formation of the 1:1 complex is more facilitated with the terdentate ketimine Schiff-base than with the bidentate $C_{12}SPM$. It is noteworthy that the reactivity of the 2:1 complex is much larger than that of the 1:1 complex in the molecular assemblies of $N^+C_5Ala2C_{14}$ and CTAB, and that the formation of the former species is more pronounced in the $N^+C_5Ala2C_{14}$ vesicle. In order that the isomerization must take place (**2** →**3** in Scheme 2), the hydrogen atom substituted on the carbon atom, interposed between the Schiff-base nitrogen and 4-carbon atom of the pyridine ring, needs to be displaced first. The polarization of the $C_4'$-H bond of a given Schiff-base chelate is important in facilitating its cleavage. Thus, the effective charge on $Cu^{II}$ must exert much effect on the reactivity. The 2:1 complex, in which the carboxylate group of the ketimine Schiff-base is free from coordination, retains positive charge on $Cu^{II}$ more effectively than the 1:1 complex, in which three coordination sites are occupied with the anionic groups. Such a charge effect provided on $Cu^{II}$ has been also claimed for the $\beta$-elimination reaction of *O*-phosphoserine with glyoxylate and copper(II) ions.[16)]

As shown in Fig. 5, the correlation between rate and $Cu^{II}$ concentration observed in the $N^+C_5His2C_{14}$ vesicle is considerably different from those in the molecular aggregates of $N^+C_5Ala2C_{14}$ and CTAB. In the light of the coordination behavior of $C_{12}SPM$ with the copper(II) ion, the primary species in a concentration range of $Cu(ClO_4)_2$ higher than $5.0\times10^{-5}$ mol $dm^{-3}$ must be the 1:1 $Cu^{II}$-ketimine chelate. However, the observed rate constant reaches a maximum at the $Cu^{II}$ concentration of $5.0\times10^{-5}$ mol $dm^{-3}$ and then falls down gradually as the $Cu^{II}$ concentration increases beyond this range. This rate profile can be understood on the basis of the coordination behavior of the imidazolyl group of $N^+C_5His2C_{14}$ with the copper(II) ion. The coordination interaction of the imidazolyl group with $Cu^{II}$ tends to stabilize the 1:1 $Cu^{II}$-ketimine chelate since the residual coordination site of $Cu^{II}$ in the 1:1 chelate is occupied with the imidazolyl group and to inhibit the formation of the corresponding 2:1 chelate. In a concentration range of $Cu(ClO_4)_2$ lower than $5.0\times10^{-5}$ mol $dm^{-3}$ where all the copper(II) ions are exclusively coordinated to the ketimine Schiff-base, the isomerization reaction of the $Cu^{II}$-ketimine chelate is catalyzed by the imidazolyl group free from coordination with the copper(II) ion (Fig. 7). We have already confirmed the catalytic assistance of the imidazolyl group as a general base in the transamination reaction of PLP with *N*-dodecyl-L-alaninamide in the $N^+C_5His2C_{14}$ vesicle.[6)] At higher concentrations of $Cu(ClO_4)_2$ beyond $5.0\times10^{-5}$ mol $dm^{-3}$, the excess copper(II) ion tends to form the $Cu^{II}$-imidazole complexes to reduce an amount of the free imidazolyl group. On this ground, the reactivity of the

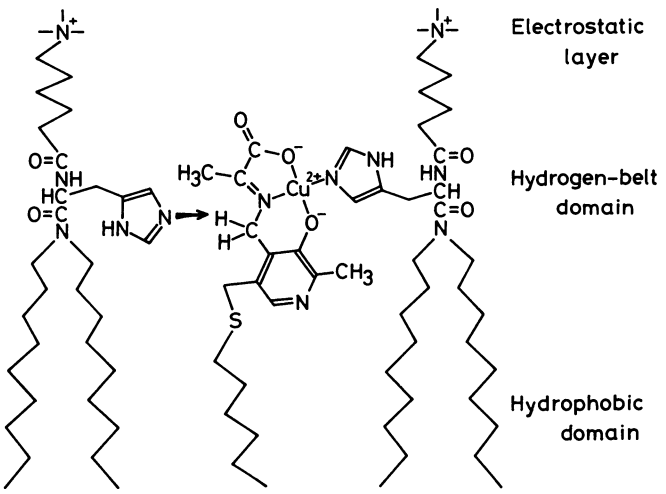


Fig. 7. Schematic representation of the isomerization mechanism for the $Cu^{II}$-ketimine complex in the $N^+C_5His2C_{14}$ vesicle.

1:1 complex in the $N^+C_5His2C_{14}$ vesicle must be facilitated by the general base catalysis of the metal-free imidazolyl group.

In conclusion, it became apparent that the copper(II)-catalyzed transamination of $C_{12}SPM$ with pyruvate in the cationic vesicles proceeds to give $C_{12}SPL$ and alanine as the final products. The detailed kinetic investigation of the isomerization of the $Cu^{II}$–ketimine to the corresponding $Cu^{II}$–aldimine clarified the following aspects. (i) In the bilayer vesicle formed with $N^+C_5Ala2C_{14}$, the formation of the reactive 2:1 (ketimine:$Cu^{II}$) complex is more favored than in the ordinary cationic micelles. (ii) The bilayer vesicle formed with the amphiphile having the histidyl residue ($N^+C_5His2C_{14}$) allows the formation of the 1:1 complex in preference to that of the 2:1 complex, and the coordination-free imidazolyl group of the amphiphile effectively catalyzes the isomerization as a general base.

The present work was supported in part by Grant-in-Aid for Scientific Research No. 58430016 from the Ministry of Education, Science and Culture.

**References**

1) E. E. Snell and S. J. Dimari, "The Enzymes," 3rd ed, ed by P. D. Boyer, Academic Press, New York (1970), Vol. 2, Chap. 7; A. E. Braunstein, "The Enzymes," 3rd ed, ed by P. D. Boyer, Academic Press, New York (1973), Vol. 9, Chap. 10.

2) D. E. Metzler, Y. Ikawa, and E. E. Snell, *J. Am. Chem. Soc.*, **76**, 648 (1954); T. C. Bruice and R. M. Topping, *ibid.*, **85**, 1480 (1963); A. E. Martell, "Advances in Enzymology," ed by A. Meister, John Wiley & Sons, New York (1982), Vol. 53, pp. 163—199.

3) Y. Murakami and H. Kondo, *Bull. Chem. Soc. Jpn.*, **48**, 541 (1975); H. Kondo, J. Kikuchi, and J. Sunamoto, *Tetrahedron Lett.*, **1983**, 2403.

4) Y. N. Belokon', V. I. Tararov, T. F. Savel'eva, and V. M. Belikov, *Makromol. Chem.*, **181**, 2183 (1980).

5) R. Breslow, M. Hammond, and M. Lauer, *J. Am. Chem. Soc.*, **102**, 421 (1980); H. Kuzuhara, T. Komatsu, and S. Emoto, *Tetrahedron Lett.*, **1978**, 3563.

6) Y. Murakami, A. Nakano, and K. Akiyoshi, *Bull. Chem. Soc. Jpn.*, **55**, 3004 (1982).

7) Y. Murakami, A. Nakano, A. Yoshimatsu, K. Uchitomi, and Y. Matsuda, *J. Am. Chem. Soc.*, in press.

8) D. E. Metzler and E. E. Snell, *J. Am. Chem. Soc.*, **77**, 2431 (1955).

9) Y. Matsushima and A. E. Martell, *J. Am. Chem. Soc.*, **89**, 1322 (1967).

10) J. Llor and M. Cortijo, *J. Chem. Soc., Perkin Trans. 2*, **1977**, 1111.

11) S. Matsumoto, Y. Karube, and Y. Matsushima, *Chem. Pharm. Bull.*, **23**, 1819 (1975).

12) N. Al-Awadi, M. S. El-Ezaby, and H. Abu-Soûd, *Inorg. Chim. Acta*, **67**, 131 (1982).

13) Y. Murakami, Y. Aoyama, and J. Kikuchi, *J. Chem. Soc., Perkin Trans. 1*, **1981**, 2809.

14) An absorption band appeared in the 620-nm range upon addition of $Cu(ClO_4)_2$ to the $N^+C_5His2C_{14}$ vesicle. This is attributable to the ligand-field band due to the coordinated copper(II) ion. However, quantitative evaluation of the stability constant for the $Cu^{II}$–$N^+C_5His2C_{14}$ complex was not possible due to insolubility of the complex in aqueous media.

15) Both 2:1 and 1:1 chelate species were assumed to have an identical molar absorption coefficient per aldimine Schiff-base unit in a similar manner as considered for the $Cu^{II}$–$C_{12}SPM$ complexes.

16) M. S. Mohan and E. H. Abbott, *Inorg. Chem.*, **17**, 3083 (1978).